Replacement of ATP with ADP Affects the Dynamic and Conformational Properties of Actin Monomer†

Balázs Gaszner,‡ Miklós Nyitrai,§ Nóra Hartvig,‡ Tamás Köszegi,|| Béla Somogyi,§,⊥ and József Belágyi*,‡

Central Research Laboratory, Research Group of the Hungarian Academy of Sciences, and Departments of Biophysics and Clinical Chemistry, University Medical School of Pécs, P.O. Box 99, H-7601 Pécs, Hungary

Received March 31, 1999; Revised Manuscript Received June 7, 1999

ABSTRACT: The effect of the replacement of ATP with ADP on the conformational and dynamic properties of the actin monomer was investigated, by means of electron paramagnetic resonance (EPR) and fluorescence spectroscopic methods. The measurement of the ATP concentration during these experiments provided the opportunity to estimate the time dependence of ADP-Mg-G-actin concentration in the samples. According to the results of the fluorescence resonance energy transfer experiments, the Gln-41 and Cys-374 residues are closer to each other in the ADP-Mg-G-actin than in the ATP-Mg-G-actin. The fluorescence resonance energy transfer efficiency increased simultaneously with the ADP-G-actin concentration and reached its maximum value within 30 min at 20 °C. The EPR data indicate the presence of an ADP-Mg-G-actin population that can be characterized by an increased rotational correlation time, which is similar to the one observed in actin filaments, and exists only transiently. We suggest that the conformational transitions, which were reflected by our EPR data, were coupled with the transient appearance of short actin oligomers during the nucleotide exchange. Besides these relatively fast conformational changes, there is a slower conformational transition that could be detected several hours after the initiation of the nucleotide exchange.

The ability of actin to polymerize into long helical filaments is fundamental to its biological function. In living cells two principal forms, the monomer and the filament forms, exist in dynamic equilibrium, which is controlled by both the properties of the actin monomer and actin binding proteins. The dynamic behavior of the actin matrix correlates with various biological activities in the cell (*1, 2*).

Understanding the details of the biological function of actin seems to be essential to describe the process of filament self-assembly and disassembly. Different experimental methods (such as phosphorescence, FRET,[1] EPR, and fluorescence quenching) were applied to investigate the effect of polymerization on the structure and dynamics of the actin monomer. Some of these studies provided experimental data suggesting that polymerization did not affect the conformational state of actin (*3*−*6*). However, in some cases the conformation of the actin monomer and the protomer incorporated into a filament structure are proved to be different (*7*−*9*).

The polymerization process usually consists of four steps, namely, activation, nucleation, elongation, and annealing. Prior to the nucleation, the conformation of the actin monomer changes, which results in a conformational state named either F-actin monomer (*10*) or G*-actin (*11*) or activated G-actin (*12*). The conformational transition can be induced by adding either K^+, Mg^{2+}, or Ca^{2+}. This conformational state appeared to be an important intermediate in the polymerization process, probably because it provides better spatial conditions for other monomers to bind in the nucleation process.

The polymerization accompanied the hydrolysis of the ATP bound to the actin. The hydrolysis of ATP occurs after the actin subunit is incorporated into the filament. The release of the inorganic phosphate (P_i) follows the hydrolysis after some time. Although the major component of the actin filament is the ADP-monomer, there are monomers near the barbed end, which contain either ATP or ADP and inorganic phosphate. On the other hand, the biological role of the ATP hydrolysis remains unclear. The presence of ATP is not essential, since the polymerization process can be also induced in the absence of ATP (in ADP-G-actin solutions) (*13*−*18*). The ATP hydrolysis is assumed to play a key role in the steady-state treadmilling of actin filaments (*19*−*26*). Carlier (*27*, *28*) suggested that the functional significance of ATP hydrolysis was that it facilitated the rapid depolymerization of actin. Jamney et al. (*29*) presented another interesting proposal. Their experimental data provided evidence that the flexibility of actin filaments polymerized from ATP- or ADP-actin monomers was different. They concluded that the energy generated by the hydrolysis of ATP

† This work was supported by grants from the National Research Foundation (OTKA T 030248, T 020117, T 023209, and F 020174) and Ministry of Health (T-06 017/1996). The Bruker EPR spectrometer used in the experiments was purchased with funds provided by the National Research Foundation (CO-123).

* Corresponding author: Telephone 36-72-324-122; Fax 36-72-315-864; E-mail belagyi@apacs.pote.hu.

‡ Central Research Laboratory.

§ Research Group of the Hungarian Academy of Sciences.

|| Department of Clinical Chemistry.

⊥ Department of Biophysics.

[1] Abbreviations: EPR, electron paramagnetic resonance; FRET, fluorescence resonance energy transfer; IAEDANS, *N*-(iodoacetyl)-*N*′-(5-sulfo-1-naphthyl)ethylenediamine; FC, fluorescein chadaverine; MSL, *N*-(1-oxyl-2,2,6,6-tetramethyl-4-piperidinyl)maleimide spin label.

10.1021/bi990748y CCC: $18.00
Published on Web 09/11/1999

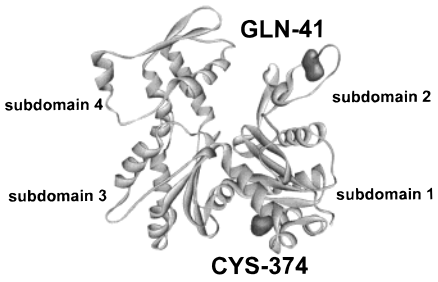

FIGURE 1: Schematic representation of the three-dimensional atomic structure of rabbit skeletal actin (*58*). The positions of the two residues (Gln-41 and Cys-374) that were modified are shown. The four subdomains of the actin monomer are also labeled on the figure. Due to the fact that the last three C-terminal residues (involving Cys-374) are not resolved in the crystal structure (*58*), the position of this residue should be taken as an approximation (the coordinates were obtained from the Brookhaven Protein Data Bank, file 1ATN).

was stored in the filament as elastic energy and available for release later on.

The investigation of the dynamic and conformational changes induced by the exchange of ATP for ADP could be important for several reasons. The effect of polymerization on the properties of actin originates from two major sources: (i) the presence of noncovalent attachment of neighboring monomers and (ii) the modification of the nucleotide content resulted from the hydrolysis of ATP. The investigation of the conformational and dynamic properties of ADP-G-actin might provide information about the latter effect. The controlled change of the nucleotide content might serve as one of the regulatory pathways in the cell, which helps to balance the self-assembly−disassembly equilibrium.

Our goal was to characterize the intra- and intermolecular changes that occurred during and after the ATP−ADP exchange in the actin monomer. The actin monomer was labeled with either spin or fluorescence probes on the Cys-374 residue and with a fluorescence reporter on the Gln-41 residue (Figure 1). We found that the exchange of ATP for ADP induced at least two distinct types of conformational changes in the actin monomer. The possible mechanisms of these processes are described in the following study.

MATERIALS AND METHODS

Reagents. KCl, $MgCl_2$, $CaCl_2$, $HClO_4$, KOH, tris(hydroxymethyl)aminomethane (Tris), *N*-(iodoacetyl)-*N*′-(5-sulfo-1-naphthyl)ethylenediamine (IAEDANS), transglutaminase (TGase), hexokinase, D-glucose, glycogen, *N*-(1-oxyl-2,2,6,6-tetramethyl-4-piperidinyl)maleimide spin label (MSL), adenosine 5′-diphosphate (ADP), adenosine 5′-triphosphate (ATP), and ethylene glycol bis(β-aminoethyl ether)-*N*,*N*,*N*′,*N*′-tetraacetic acid (EGTA) were obtained from Sigma Chemical Co. (St. Louis, MO). β-Mercaptoethanol (MEA) was obtained from Merck (Darmstadt, Germany), the fluorescein chadaverine (FC) from Molecular Probes (Eugene, OR), and NaN_3 from Fluka (Switzerland).

Protein Preparation. Acetone-dried powder of rabbit skeletal muscle was obtained as described earlier (*30*). Rabbit skeletal-muscle actin was prepared according to the method of Spudich and Watt (*31*) with a slight modification introduced by Mossakowska et al. (*32*) and stored in a buffer containing 2 mM Tris-HCl (pH 8.0), 0.2 mM ATP, 0.1 mM $CaCl_2$, and 0.02% NaN_3 (buffer A). The concentration of G-actin was determined spectrophotometrically by using the absorption coefficient of 0.63 mg mL^{-1} cm^{-1} at 290 nm (*33*) with a Shimadzu UV-2100 type spectrophotometer. Relative molecular mass of 42 300 was used for G-actin (*34*). The bound Ca^{2+} was replaced by Mg^{2+} in the actin monomer by means of the method of Strzelecka-Golaszewska et al. (*6*). EGTA and $MgCl_2$ were added to reach the final concentrations of 0.2 and 0.1 mM, and the solution was stirred for 10 min at room temperature. The ATP was replaced by ADP as described by Drewes and Faulstich (*35*): 1 mM of ADP and 30 units/mL hexokinase and 2.5 mM glucose were added to a Mg-ATP-G-actin solution. The addition of hexokinase and glucose was necessary, since ADP stocks commercially available were inhomogeneous and the original buffer contained 0.2 mM ATP. The dissociation constant of either ATP or ADP in actin falls into the subnanomolar range (*36*). Therefore, it is reasonable to assume that the concentration of actin monomers with no bound nucleotide is negligible under these experimental conditions.

Labeling of Actin. The reactive cysteine residue, Cys-374, of the actin was labeled with IAEDANS as described by Miki et al. (*37*). The solution of F-actin (2 mg/mL) was incubated with a 10-fold molar excess of the dye for 1 h at room temperature. The labeling was terminated by adding 1 mM MEA. The unbound IAEDANS was removed from the samples by centrifugation at 100000*g* for 2 h at 4 °C. The pellet was gently homogenized with a Teflon homogenizer, and the homogenate was dialyzed against buffer A overnight at 4 °C. After the dialysis the samples were clarified at 100000*g* for 1 h just before the spectroscopic experiments.

The labeling of Gln-41 with FC was carried out according to the method of Takashi (*38*). G-actin was incubated with a 10-fold molar excess of the dye in the presence of 1 mg/mL TGase. The labeling was carried out for 16 h at 4 °C. Following the incubation the sample was polymerized by adding KCl and $MgCl_2$ to final concentrations of 100 and 2 mM, respectively. The unreacted FC was removed and the actin was dialyzed as described in the case of IAEDANS labeling.

The concentration of the IAEDANS and FC in the protein solution was determined by using the absorption coefficient of 6100 M^{-1} cm^{-1} at 336 nm (*39*) and 75 500 M^{-1} cm^{-1} at 493 nm (*40*). The extent of labeling for IAEDANS and FC was determined to be 0.83 ± 0.02 and 0.8 ± 0.03 mol/mol of actin, respectively.

The Cys-374 of the actin was labeled with MSL in filamentous form as described earlier (*32*). Spin label (1.2 mol/mol of actin monomer) was reacted for 1 h at 0 °C. Unreacted labels were removed as described in the case of IAEDANS labeling procedure. The degree of labeling with MSL was 0.91 ± 0.07 mol/mol of actin.

Fluorescence Experiments. The fluorescence properties of the labeled actin samples (23−25 μM) were measured with a Perkin-Elmer LS50B spectrofluorometer. When the time dependence of the fluorescence of IAEDANS was investigated, the samples were excited at 350 nm, and the emission was detected at 480 nm. The optical slits were set at 3 nm in both the excitation and emission sides. The fluorescence intensity of the Ca-ATP-G-actin sample was monitored before and after the addition of 0.1 mM $MgCl_2$ and 0.2 mM EGTA. When the cation exchange was complete, which was evidenced by the saturation of intensity increase, the appropriate amounts of ADP, hexokinase, and glucose were

also added to the solution. The fluorescence intensity of the IAEDANS was followed routinely for 1 h, and in some cases after 12 h of incubation at room temperature. To characterize the possible undesired effect of the compounds used for the nucleotide exchange, experiments were carried out when only either ADP, or hexokinase, or glucose was added to the samples.

The efficiency (E) of the fluorescence resonance energy transfer (FRET) between the IAEDANS (donor, attached to the Cys-374) and FC (acceptor at the Gln-41) was calculated from the fluorescence intensity in the presence and absence of acceptor as

$$E = (F_{DA}/F_D)/\beta \quad (1)$$

where F_{DA} and F_D is the fluorescence intensity of the donor in the presence and absence of acceptor, respectively, and β is the labeling ratio of the acceptor. The intensities used for this calculation were measured similarly as described above, except that the emission of the IAEDANS was detected at 470 nm so that the contribution of the fluorescent acceptor could be avoided. The fluorescence data were corrected for the inner filter effect, for the donor concentration in the samples, and also for the small dilution of the samples inserted by adding materials used for the cation and nucleotide exchange.

The steady-state fluorescence anisotropy of IAEDANS was also measured as a function of time after the nucleotide exchange. The fluorescence anisotropy was calculated from the polarized emission components (F_{VV}, F_{VH}, F_{HV}, and F_{HH}, where the subscripts indicate the orientation of the excitation and emission polarizers) as

$$r = (F_{VV} - GF_{VH})/(F_{VV} + 2GF_{VH}) \quad (2)$$

where $G = F_{HV}/F_{HH}$. The excitation wavelength was 350 nm and the emission wavelength was 480 nm. The slits were set to 3 nm.

The fluorescence lifetime and emission anisotropy decay of IAEDANS-actin (23−25 μM) were measured at 25 °C. These measurements were performed according to the frequency cross-correlation method by means of an ISS K2 multifrequency phase fluorometer (ISS Fluorescence Instrumentation, Champaign, IL). Glycogen solution prepared freshly was used as a reference (lifetime = 0 ns) in the fluorescence lifetime experiments. The data were analyzed by the ISS187 decay analysis software. The goodness of fitting was determined from the value of the reduced χ^2 (*41*). The excitation light source was a 300-W Xe arc lamp. The excitation light intensity was modulated with a double-crystal Pockels cell. Excitation wavelength was set to 350 nm and the emission was monitored through a KV 370 high-pass filter. The modulation frequency was changed in 10 or 15 steps (linearly distributed on a logarithmic scale) from 2 to 80 MHz and from 2 to 120 MHz in fluorescence lifetime and anisotropy decay measurements, respectively.

In fluorescence lifetime measurements all data were fit to double-exponential decay curves, when a constant, frequency-independent error was assumed in both phase angle (±0.200°) and modulation ratio (±0.004). The same standard errors were also used in anisotropy decay measurements.

In two-exponential lifetime analysis the average fluorescence lifetimes were calculated as described by Lakowicz (*41*):

$$\tau_{av} = (\tau_1^2\alpha_1 + \tau_2^2\alpha_2)/(\tau_1\alpha_1 + \tau_2\alpha_2) \quad (3)$$

where τ_{av} is the average fluorescence lifetime and α_i and τ_i are the individual amplitudes and lifetimes, respectively.

The anisotropy is expected to decay as a sum of exponentials (*42*). Accordingly, the experimental data were fitted to a double-exponential function:

$$r(t) = r_0[g_1 \exp(-t/\phi_1) + g_2 \exp(-t/\phi_2)] \quad (4)$$

where r_0 is the limiting anisotropy and ϕ_1 and ϕ_2 are the two rotational correlation times with amplitudes g_1 and g_2, respectively.

EPR Experiments. Conventional EPR measurements were performed by means of a Bruker ESP 300E (Bruker, Germany) spectrometer, and 100 kHz field modulation, 0.1−0.2 mT amplitude, a 10 mT field scan, and 20 mW microwave power were used. The concentration of the samples in EPR measurements was 50 μM. Spectra were recorded at temperatures between 10 and 35 °C. The rotational correlation time (τ_R) for monomer actin was calculated as proposed by Goldman et al. (*43*):

$$\tau_R = 5.4 \times 10^{-10}\,(1 - A'_{ZZ}/A_{ZZ})^{-1.36} \quad (5)$$

where $2A'_{ZZ}$ and $2A_{ZZ}$ are defined as the hyperfine splitting between the outer extrema of the experimental spectrum and the rigid limit spectrum, respectively.

ATP Measurements. The measurements of ATP concentrations were carried out according to the firefly luciferin/luciferase system by means of a Biolumat LB 9507 (Berthold, Germany) luminometer. These experiments were performed under the same experimental conditions as those in the spectroscopic measurements in the presence or the absence of actin monomers. After hexokinase and glucose were added to buffer A, aliquots (0.1 mL) were mixed with 0.1 mL of 1 M $HClO_4$ and centrifuged at 3000*g* for 3 min. The supernatants (0.15 mL) were mixed with 0.1 mL of 2.3 M KOH. After centrifugation, the neutralized samples were diluted 2000 times and the measurements were done with internal standardization (*44*).

RESULTS

The effect of the replacement of ATP with ADP on the conformational properties of the actin monomer was studied by conventional EPR spectroscopy. Maleimide spin labels (MSL) were covalently attached to the Cys-374 residue of the actin monomer and performed rotational motion, which is characteristic of a strongly immobilized label in ATP-G-actin (Figure 2b). The amount of labels bound to the weakly immobilizing sites was less than 5%, which indicates selective labeling procedure. This fraction was estimated by double-integrating the narrow, high-field line in the F-actin spectrum. The hyperfine splitting constant ($2A'_{ZZ}$, the distance between the outermost extrema) was 6.40 mT at 20 °C for the ATP-G-actin. This value corresponds to a rotational correlation time of 19.6 ns, which is in good accordance with our previous data (*45*). The time and temperature dependence

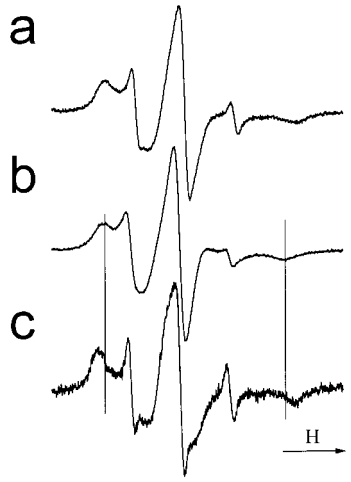

FIGURE 2: Effect of nucleotide exchange on the conventional EPR spectra of MSL labeled Mg-ATP-G-actin. The spectra were recorded before (b) and 30 min after (a) the initiation of the nucleotide exchange. To separate the two actin populations in the composite spectrum (a), the EPR spectrum of Mg-ATP-G-actin (b) was subtracted from the EPR spectrum (a). The difference spectrum (c) characterizes a new actin population with increased hyperfine splitting constant of 6.779 mT. The fraction of this state is 0.5. The scan width in each spectrum is 10 mT.

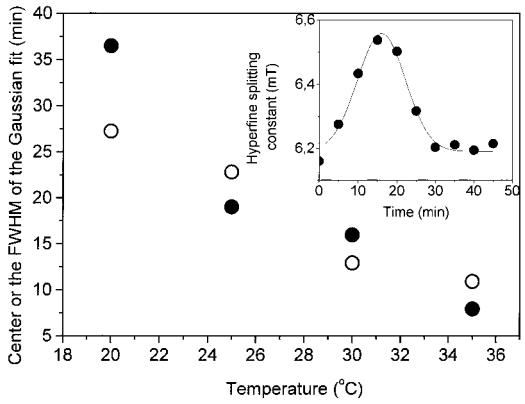

FIGURE 3: Effect of nucleotide exchange on the hyperfine splitting constant ($2A'_{ZZ}$) of Mg-ATP-G-actin at temperatures between 20 and 35 °C. The time dependence of $2A'_{ZZ}$ was approximated by a Gaussian function, the maximum value (●) and the full width at half-maximum (fwhm) (○) of the Gaussian curves were plotted against temperature. The inset shows a representative plot of change in the hyperfine splitting vs time at 30 °C. Zero time corresponds to the initiation of the nucleotide exchange.

of the hyperfine splitting constant was monitored after the initiation of ATP−ADP exchange in the actin monomer.

The effect of the nucleotide exchange on the hyperfine splitting constant was negligible below 20 °C. However, we detected an early increase of $2A'_{ZZ}$, which was followed by a rapid decrease, when the experiments were performed between 20 and 35 °C (see, e.g., inset in Figure 3). The time dependence of the hyperfine splitting constant was approximated by a Gaussian function during this period (inset in Figure 3). The maximum value and the full width at half-maximum (fwhm) of these curves versus temperature indicate a temperature-dependent appearance of a transient actin population (Figure 3). Furthermore, the species observed at the end of the decreasing process existed at a longer time scale and could be detected even after 12 h. The rotational correlation time was 36.1 ns at the maximum value of $2A'_{ZZ}$ (6.51 ± 0.03 mT, $n = 4$), which exceeds the τ_R of a single

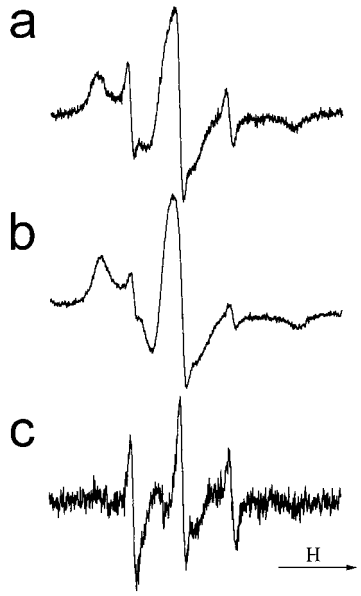

FIGURE 4: Conventional EPR spectra of MSL-Mg-G-actin and MSL-Mg-F-actin. The spectrum of Mg-actin filaments (b) was subtracted from the residual spectrum, which is in Figure 2c (a), obtained from the Mg-ATP-G-actin spectrum recorded 30 min after the initiation of the nucleotide exchange. The difference spectrum (c) indicates a spin label population with little restricted rotational motion. The EPR data indicate that during the early phase of the nucleotide exchange there is a structural change in the actin sample, which results in an F-actin-like population. The scan width in each spectrum is 10 mT.

monomer actin. The transient change of the spectral parameters and the τ_R data indicate more than one actin population, which can be distinguished by different rotational mobility. To separate these populations, we subtracted the spectrum of ATP-G-actin measured at 20 °C (Figure 2b) from the composite ATP−ADP spectrum obtained 30 min after the nucleotide exchange (Figure 2a). Replacing ATP with ADP resulted in an actin population characterized by an increased hyperfine splitting constant of 6.779 ± 0.04 mT ($n = 5$, mean $\pm$ SD) which is similar to the value obtained on F-actin (6.787 mT) (Figure 4).

The ratio of the two population was 0.500 ± 0.086 ($n = 4$), which was calculated from the double integrals of the composite spectra. The results indicate that during the early phase of the nucleotide exchange there is a structural change in the actin sample, which results in an F-actin-like population (Figure 4), and at the maximum of the hyperfine splitting constant the two populations are nearly equal (Figure 2). When the F-actin spectrum was subtracted from the composite spectrum, the hyperfine splitting constant of the residual spectrum approximated that of the monomer actin (6.307 mT), and the double integral of this spectrum was 54.3% of the composite spectrum, which supports the suggestions about the presence of actin oligomers during the exchange process. The fraction of the weakly immobilized spin labels follows a growing tendency at a longer time scale. The increased amount of labels with little restricted rotational motion reflects the well-described denaturation characteristic of the ADP-Mg-G-actin monomers (*46*, *47*).

Fluorescence experiments were also carried out so that more information could be obtained about the underlying intramolecular events during the nucleotide exchange in actin monomers. The steady-state fluorescence anisotropy of

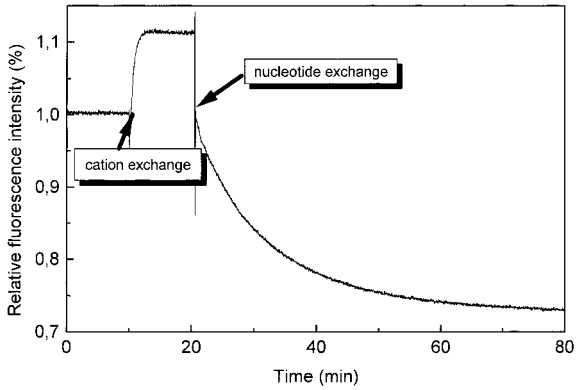

FIGURE 5: Time dependence of the fluorescence emission of IAEDANS (attached to Cys-374) during the cation and nucleotide exchange at 20 °C. Arrows indicate the initiation of these processes. The excitation and emission wavelengths were 350 and 480 nm, respectively. The optical slits were set to 3 nm at both sides.

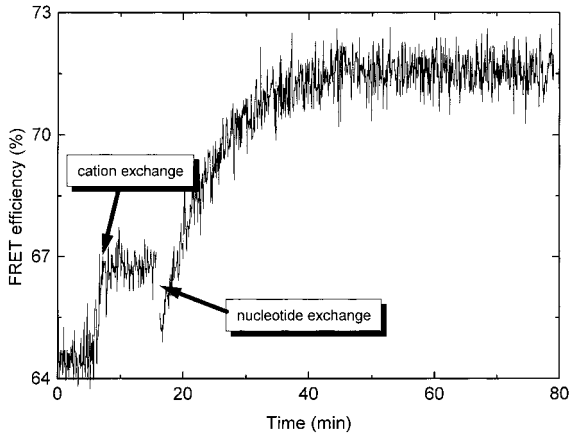

FIGURE 6: Time kinetics of the fluorescence resonance energy transfer efficiencies during the $Ca^{2+}-Mg^{2+}$ and ATP−ADP exchange at 20 °C. Arrows indicate the initiation of the cation exchange and nucleotide exchange processes. The fluorescence emission of the IAEDANS was measured either in the presence or in the absence of its acceptor (FC) with excitation and emission wavelengths of 350 and 470 nm, respectively. The optical slits were set to 3 nm. The transfer efficiency was calculated from these quantities as described in the Materials and Methods section.

IAEDANS, covalently attached to the Cys-374 residue of the actin monomer, was not sensitive to the nucleotide exchange within the first 60 min. On the other hand, the exchange of Ca^{2+} for Mg^{2+} induced an about 10% increase of the fluorescence intensity of this fluorophore (Figure 5), in agreement with earlier publications (*48*). The fluorescence intensity of IAEDANS also proved to be sensitive to the nucleotide exchange in Mg-G-actin (Figure 5) in accordance with the results of Frieden and Patane (*49*). Adding ADP, hexokinase, and glucose (see Materials and Methods) to Mg-ATP-G-actin resulted in an about 35% decrease of the fluorescence emission within 60 min at 20 °C. One part (8−9%) of this 35% drop in the fluorescence intensity is due to the change of the optical properties of the protein solution, which is evidenced by the separate addition of the individual components used to initiate the nucleotide exchange (i.e., hexokinase, glucose, and ADP) in control experiments (see also Materials and Methods). This 8−9% decrease occurred promptly after the addition of these compounds. The fluorescence intensity of IAEDANS showed a decreasing tendency even 12 h after the initiation of the replacement of ATP with ADP. To characterize the time kinetics of this decrease in the fluorescence emission, the curves obtained experimentally (Figure 5) were fitted, when first-, second-, and third-order exponential decay functions were assumed. The analysis resulted in the best fit when second-order exponential decay was assumed, which indicated that there were two major processes contributing to the observed intensity changes. The first component of this analysis has a lifetime of approximately 25 min, which might indicate the relatively rapid conformational changes. The lifetime of the second component is much longer (couple of hours) and could not be well determined, probably due to the relatively short duration of the experiments. Accordingly, there is a long-time conformational transition induced by the replacement of ATP with ADP. This long conformational transition is likely to be the same as the one described by Drewes and Faulstich (*35*).

In the fluorescence resonance energy transfer experiments the IAEDANS served as a donor and the acceptor was FC, which was attached to the Gln-41 residue of subdomain 2. The transfer efficiency between these probes increased slightly from 65% to 67% at 20 °C as a result of exchange of Ca^{2+} with Mg^{2+} in the ATP-G-actin (Figure 6), in good agreement with our recent observation (*50*). After the addition of appropriate amounts of ADP, hexokinase, and glucose, the transfer efficiency continued to increase up to 72% in Mg-G-actin at 20 °C (Figure 6). This is consistent with the results of Kim et al. (*51*). They found that the FRET efficiency between the Trp residues of the subdomain 1 and the fluorescence probe (dansyl ethylenediamine, DED) located at the Gln-41 residue of the subdomain 2 was greater in ADP-G-actin than in ATP-G-actin. The increase of the IAEDANS−FC transfer efficiency was completed within 30 min in our experiments (Figure 6).

The fluorescence lifetime and rotational correlation time of IAEDANS was also determined. The duration of such experiments is about 15−20 min under these experimental conditions, which means a relatively poor time resolution. Therefore, the obtained data should be considered indicative only in a qualitative manner. The average fluorescence lifetime of IAEDANS in Mg-ATP-G-actin was found to be 19.1 ± 0.3 ns, which is in agreement with our earlier data (*45*). Further lifetime experiments were started at 10, 35, and 60 min after the start of the nucleotide exchange. According to these experiments, the average fluorescence lifetime decreased to 17.4 ± 0.4, 16.7 ± 0.4, and 16.4 ± 0.3 ns, respectively. This decreasing tendency is consistent with the time kinetics of the steady-state fluorescence emission of IAEDANS. The shorter rotational correlation times fall into the range of 0.5−0.8 ns and might be attributed to the rotational mobility of the IAEDANS. The longer rotational correlation time of Mg-ATP-G-actin was 28 ± 2 ns. The fluorescence anisotropy decay experiments were also started 10, 35, and 60 min after the nucleotide exchange was initiated. In the analysis of these results we assumed that there were two kinds of actin populations. One part of the actin was still in monomeric form having the same fluorescence lifetime as the Mg-ATP-G-actin. Another part was already converted to a new species. This part of the actin could be characterized by a fluorescence lifetime, which was measured 60 min after the initiation of the nucleotide exchange. Following this strategy, we obtained a longer

Table 1: Time Dependence of the ATP Content of the Sample[a] as a Function of Temperature in the Presence and Absence of Actin

temp (°C)	actin	time (min) 0.5	1	2	4	6	8	10	12
20	−	0.41	0.44	0.42	0.47	0.56	0.57	0.44	0.46
5	−	0.38	0.43	0.36	0.40	0.48	0.51	0.43	0.48
20	+	15.94	15.22	14.54	11.96	10.36	9.19	8.03	7.35
5	+	16.78	16.74	15.56	14.43	12.84	12.45	10.81	10.41

[a] Expressed as a percentage of the initial ATP concentration.

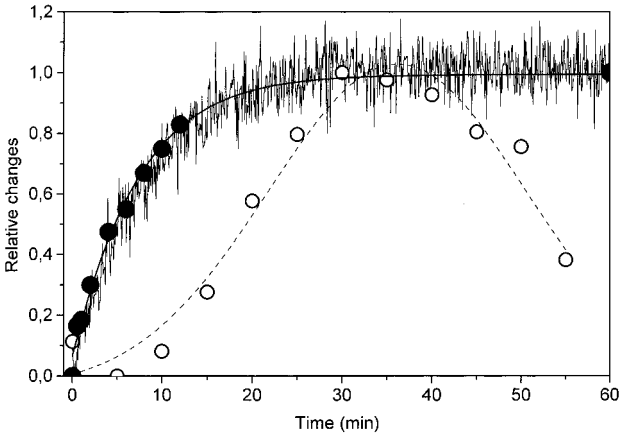

FIGURE 7: Comparison between the relative changes in the FRET efficiency, the hyperfine splitting constant (○), and the calculated ADP-actin concentrations (●). The relative changes were calculated in a way that the actual change was compared to the largest observed change of the given parameter. Data were plotted as a function of time, where zero time is the initiation of the nucleotide exchange. The solid line corresponds to the fit to the ADP-actin concentration and the dotted line is the Gaussian fit to the EPR data. All the experiments were carried out at 20 °C (see also Materials and Methods).

rotational correlation time of the new actin population, which was 52 ± 5 ns. The relative amplitude of this correlation time decreases from 0.6 (measured after 10 min) to 0.47 (35 min) and 0.42 (60 min).

We also verified the efficiency of the nucleotide exchange by measuring the total ATP concentration in either the presence or absence of actin monomers. This was performed by applying the same experimental conditions as those in the spectroscopic measurements. In the absence of actin the initial 200 μM ATP concentration was reduced to a negligible level within 30 s at both 5 and 20 °C (Table 1). However, in the presence of the actin monomers a similarly fast decrease of the ATP concentration was followed by slower ATP consumption (Table 1). The decrease of the ATP concentration was 16% slower at 5 °C than at 20 °C (Table 1). The different time kinetics of the ATP concentrations in the presence and absence of actin are very likely to be attributed to the bound fraction of the ATP. Accordingly, the slower phase of the ATP concentration vs time can be considered as a good measure of the actin-bound ATP and, therefore, the ATP-G-actin concentration. Since the ATP-G-actin and total actin concentrations are known, the increase in the ADP-G-actin concentration can be calculated (Figure 7).

DISCUSSION

Formation and rearrangement of actin networks are regulated by many factors within a cell. The nucleotide-dependent states of actin can significantly affect this process during the assembly and disassembly of cytoplasmic structure. In this work the influence of the exchange of ATP for ADP on the conformational and dynamic properties of the actin monomer was studied by applying EPR and fluorescence spectroscopic methods. The EPR data provided evidence for the presence of a transient actin population during the nucleotide exchange (Figures 2 and 3). The rotational correlation time characteristic of this actin population is longer than the one measured on ATP-Mg-G-actin. Earlier EPR experiments showed that MSL was rigidly attached to the Cys-374 residue of the actin, and the rotational correlation time of the label reflected the motion of the whole monomer or a larger domain of it (*32*, *53*). The apparent rotational correlation time (36.1 ns) observed at the maximum value of $2A'_{ZZ}$ exceeds the τ_R of a single monomer. Therefore, one can conclude that an internal conformational change in the monomer itself cannot explain the change of the hyperfine splitting constant. This assumes that there is a substantial oligomer concentration in the samples during the ATP−ADP exchange. Considering the time kinetics of the hyperfine splitting constant (Figure 3), the insensitivity of the steady-state fluorescence anisotropy to the nucleotide exchange (*52*), and the results of Drewes and Faulstich (*35*), we can exclude the presence of actin filaments during the nucleotide exchange. Accordingly, the nucleotide-modulated changes in the hyperfine splitting constant, which occurs after the initiation of nucleotide exchange, are probably the consequence of the presence of the short actin oligomers (Figure 4). This oligomer population exists transiently (Figure 3). The observation that the mixture of ATP-actin and ADP-actin monomers nucleates better than homogeneous solutions of either monomer supports this explanation (*54*).

The existence of the transient oligomer population was temperature-dependent and its time kinetics could be characterized on a time scale of minutes (Figure 3). The ATP concentration measurements indicate that the nucleotide exchange procedure itself cannot be the rate-limiting step of this time dependence (Table 1). The change in the temperature influences the rate of the oligomerization, which results in the fact that the transient change in actin population is slower at lower temperatures (Figure 3). However, the conformational transitions induced by nucleotide exchange at temperatures below 20 °C were probably concealed by the superimposed effect of temperature on the hyperfine splitting constant.

In the FRET measurements a conformational change was also detected after the initiation of the replacement of ATP with ADP (Figure 6). The transfer efficiency increased during ATP−ADP exchange and reached its maximum value (72%) within 30 min at 20 °C. Therefore, one can conclude that there is conformational transition in the actin monomer, which brings the two labeled residues (i.e., Gln-41 and Cys-374) closer to each other. This conformational change is probably the same as the one reflected by the faster component (characterized by a lifetime of about 25 min) in the analysis of the time dependence of the IAEDANS emission.

In contrast to the time dependence of the hyperfine splitting constant, the change of the FRET efficiency is not transient (Figure 7). This observation indicates that the increase of the FRET efficiency is not the consequence of

the proposed formation of oligomers. The insensitivity of the FRET efficiency to the oligomerization suggests that the spatial arrangement of monomers within these oligomers does not induce an effective interprotomer energy transfer. It is known that the Gln-41 residue in subdomain 2 and the Cys-374 residue in subdomain 1 are close to each other within the actin filament (*55*, *56*). Accordingly, in the oligomers generated during the ATP−ADP exchange the connection sites between adjacent monomers are different from the ones along the long-pitch helix in the actin filaments.

Comparing the time dependence of the ADP-Mg-actin concentration with the obtained spectroscopic parameters provides further information regarding the intramolecular or intermolecular events occurring during the nucleotide exchange. The FRET efficiency increases simultaneously with the ADP-Mg-G-actin concentration (Figure 7), which indicates that approaching of Gln-41 to Cys-374 residue occurs promptly after the nucleotide exchange. On the other hand, the increase of the hyperfine splitting constant is in delay compared to the ADP-Mg-actin concentration, which indicates that the formation of oligomers happens on a slower time scale, after the intramonomer conformational transition reflected by the FRET data (Figure 7).

According to other studies the steady-state fluorescence anisotropy of the IAEDANS increased in pPDM cross-linked actin dimer (0.22), compared to the value (0.16) obtained on actin monomer (*57*). Therefore, the insensitivity of the anisotropy of the IAEDANS to the replacement of ATP with ADP, during which the formation of oligomers is suggested, requires further explanation. One might assume that the oligomers generated under different experimental conditions could exhibit significantly different structures of actin monomers. So, it is possible that the connecting sites of actin monomers in the oligomers during the ATP−ADP exchange differ from the sites in the pPDM cross-linked dimers that were described by Chaussepied and Kasprzak (*57*). In this case it is reasonable to assume that in our experiments the oligomerization process affects differently the environment of the Cys-374 and, thus, the value of the fluorescence anisotropy of IAEDANS. In contrast to the steady-state anisotropy of the fluorescence label, the spectroscopic properties of the EPR probe (connected to the same residue, Cys-374) were sensitive to the nucleotide exchange. It is very likely that this apparent contradiction is due to the fact that different reporter molecules and methods were applied. The dynamics of the probes attached to the proteins depends on probe size and attaching linkage. Therefore it is possible that the rigidly attached MSL is able to reflect the change of the global motion that is expected during oligomer formation, while the steady-state anisotropy of a fluorescent probe is relatively insensitive to the oligomerization. However, even in this case, the fluorescence anisotropy decay experiments should detect the presence of oligomers. The longer rotational correlation time resolved for Mg-ATP-G-actin (28 ± 2 ns) is characteristic of the overall rotational motion of the actin monomer (*45*). The presence of oligomers is expected to increase the value of this parameter. According to the time-resolved anisotropy experiments there is an actin population during the nucleotide exchange that can be characterized by a longer rotational correlation time of 52 ± 5 ns. Although these rotational correlation times should not be taken as quantitatively robust data (see Results section), one can conclude that the presence of a new actin population with substantially slower rotational mobility is evidenced. Furthermore, the contribution of this population to the observed anisotropy decay is decreasing with time in qualitative accordance with the EPR data.

SUMMARY

In light of these spectroscopic data, there are at least two kinds of conformational transitions in the actin monomer after the initiation of nucleotide exchange. There is a rapid conformational change where the Gln-41 and Cys-374 residues come closer to each other. This new conformational state provides the structural basis for the generation of an oligomer population. In these oligomers the connection sites between adjacent monomers are different from the ones along the long-pitch helix in the actin filaments. Further conformational transitions lead to the decrease of the concentration of oligomers. On the other hand there is a slower conformational change in the actin monomer that could be detected even several hours after the start of the nucleotide exchange (*35*). These results emphasize the importance of the nature of the nucleotide (ATP or ADP) bound to the monomer actin in the regulation of actin polymerization.

REFERENCES

1. Carlier, M.-F. (1991) *Curr. Opin. Cell Biol. 3*, 12−17.
2. Reisler, E. (1993) *Curr. Opin. Cell Biol. 5*, 41−47.
3. Miki, M. (1991) *Biochemistry 30*, 10878−10884.
4. O'Donoghue, S. I., Hambly, B. D., and dos Remedios, C. G. (1992) *Eur. J. Biochem. 205*, 591−601.
5. Strambini, G. B., and Lehrer, S. S. (1991) *Eur. J. Biochem. 195*, 645−651.
6. Strzelecka-Golaszewska, H., Moraczewska, J., Y., K. S., and Mossakowska, M. (1993) *Eur. J. Biochem. 211*, 731−742.
7. Tao, T., and Cho, J. (1979) *Biochemistry 18*, 2759−2765.
8. Hild, G., Nyitrai, M., Gharavi, R., Somogyi, B., and Belágyi, J. (1996) *J. Photochem. Photobiol B: Biol. 35*, 175−179.
9. Nyitrai, M., Hild, G., Belágyi, J., and Somogyi, B. (1999) *J. Biol. Chem. 274*, 12996−13001.
10. Rich, S. A., and Estes, J. E. (1976) *J. Mol. Biol. 104*, 777−792.
11. Rouayrenc, J. F., and Travers, F. (1981) *Eur. J. Biochem. 116*, 73−77.
12. Shu, W. P., Wang, D., and Stracher, A. (1992) *Biochem. J. 283*, 567−573.
13. Cooke, R., and Murdoch, L. (1973) *Biochemistry 12*, 3927−3932.
14. Cooke, R. (1975) *Biochemistry 14*, 3250−3256.
15. Hayashi, T., and Rosenbluth, R. (1962) *Biochem. Biophys. Res. Commmun. 8*, 20−23.
16. Higashi, S., and Oosawa, F. (1965) *J. Mol. Biol. 12*, 843−865.
17. Iyengar, M. R., and Weber, H. H. (1964) *Biochim. Biophys. Acta 86*, 543−553.
18. Pollard, T. D. (1984) *J. Cell Biol. 99*, 769−777.
19. Wang, Y. L., and Taylor, D. L. (1981) *Proc. Natl. Acad. Sci. U.S.A. 78*, 5503−5507.
20. Wegner, A. (1970) *J. Mol. Biol. 109*, 139−150.
21. Wegner, A. (1982) *J. Mol. Biol. 161*, 607−615.
22. Wegner, A., and Isenberg, G. (1983) *Proc. Natl. Acad. Sci. U.S.A. 30*, 4922−4925.
23. Pollard, T. D., and Mooseker, M. S. (1981) *J. Cell Biol. 88*, 654−659.
24. Hill, T. L., and Kirschner, M. W. (1982) *Int. Rev. Cytol. 78*, 1−125.
25. Bonder, E. M., Fishkind, D. J., and Mooseker, M. S. (1983) *Cell 34*, 491−501.
26. Neuhaus, J.-M., Wanger, M., Keiser, T., and Wegner, A. (1983) *J. Muscle Res. Cell Motil. 4*, 507−527.

27. Carlier, M.-F. (1990) *Adv. Biophys. 26*, 51−73.
28. Carlier, M.-F. (1991) *J. Biol. Chem. 266*, 1−4.
29. Jamney, P. A., Hvidt, S., Oster, G. F., Lamb, J., Stossel, T. P., and Hartwig, J. H. (1990) *Nature 347*, 95−99.
30. Feuer, G., Molnár, F., Pettkó, E., and Straub, F. B. (1948) *Hung. Acta Physiol. 1*, 150−163.
31. Spudich, J. A., and Watt, S. (1971) *J. Biol. Chem. 246*, 4866−4871.
32. Mossakowska, M., Belágyi, J., and Strzelecka-Golaszewska, H. (1988) *Eur. J. Biochem. 175*, 557−564.
33. Houk, W. T., and Ue, K. (1974) *Anal. Biochem. 62*, 66−74.
34. Elzinga, M., Collins, J. H., Kuehl, W. M., and Adelstein, R. S. (1973) *Proc. Natl. Acad. Sci. U.S.A. 70*, 2687−2691.
35. Drewes, G., and Faulstich, H. (1991) *J. Biol. Chem. 266*, 5508−5513.
36. Cheesman, D. F., and Priston, A. (1972) *Biochem. Biophys. Res. Commun. 48*, 552−558.
37. Miki, M., dos Remedios, C. G., and Barden, J. A. (1987) *Eur. J. Biochem. 168*, 339−345.
38. Takashi, R. (1988) *Biochemistry 27*, 938−943.
39. Hudson, E. N., and Weber, G. (1973) *Biochemistry 12*, 4154−4161.
40. Lorand, L., Parameswaran, K. N., Velasco, P. T., Hsu, L. K.-H., and Siefring, G. E., Jr. (1983) *Anal. Biochem. 131*, 419−425.
41. Lakowicz, J. R. (1983) in *Principles of Fluorescence Spectroscopy* (Lakowicz, J. R., Ed.) pp 52−59, Plenum Press, New York and London.
42. Belford, G. G., Belford, R. L., and Weber., G. (1972) *Proc. Natl. Acad. Sci. U.S.A. 69*, 1392−1393.
43. Goldman, S. A., Bruno, G. V., and Freed, J. H. (1972) *J. Phys. Chem. 76*, 1858−1860.
44. Köszegi, T., Kellermayer, M., Kövecs, F., and Jobst, K. (1988) *J. Clin. Chem. Clin. Biochem. 26*, 599−604.
45. Nyitrai, M., Hild, G., Belágyi, J., and Somogyi, B. (1997) *Biophys. J. 73*, 2023−2032.
46. Grubhofer, N., and Weber, H. H. (1961) *Z. Naturforsch. 16b*, 435−444.
47. Nowak, E. H., Strzelecka-Golaszewska, H., and Goody, R. (1988) *Biochemistry 27*, 1785−1792.
48. Frieden, C., Lieberman, D., and Gilbert, H. R. (1980) *J. Biol. Chem. 255*, 8991−8993.
49. Frieden, C., and Patane, K. (1985) *Biochemistry 24*, 4192−4196.
50. Nyitrai, M., Hild, G., Lakos, Z., and Somogyi, B. (1998) *Biophys. J. 74*, 2474−2481.
51. Kim, E., Motoki, M., Seguro, K., Muhlrad, A., and Reisler, E. (1995) *Biophys. J. 69*, 2024−2032.
52. Kasprzak, A. A. (1994) *Biochemistry 33*, 12456−12462.
53. Thomas, D. D., Seidel, J. C., and Gergely, J. (1979) *J. Mol. Biol. 132*, 257−273.
54. Pantaloni, D., Carlier, M. F., and Korn, E. D. (1985) *J. Biol. Chem. 260*, 6572−6578.
55. Milligan, R. A., Whittaker, M., and Safer, D. (1990) *Nature 348*, 217−221.
56. Holmes, K. C., Popp, D., Gebhard, W., and Kabsch, W. (1990) *Nature 347*, 44−49.
57. Chaussepied, P., and Kasprzak, A. A. (1989) *Nature 342*, 950−953.
58. Kabsch, W., Mannherz, H. G., Suck, D., and Pai, E. F. (1990) *Nature 347*, 37−43.

BI990748Y